MAGNETICS REDUCERS STUDY AND THEIR INSERTION IN PERMANENT MAGNET SYNCHRONOUS MACHINES

***AGBOKPANZO Richard Gilles[1], d'ALMEIDA Renaud[2], HOUNGAN Aristide[1]
and ESPANET Christophe[3]**

[1]*Université Nationale des Sciences, Technologies Ingénierie et Mathématiques d'Abomey, Ecole Normale Supérieure de l'Enseignement Technique (ENSET) de Lokossa, LARPET, Bénin*
[2]*Ecole Polytechnique d'Abomey-Calavi, Université d'Abomey-Calavi, Bénin*
[3]*Département Énergie, Femto-St, CNRS, Univ. Bourgogne Franche-Comté, F90000 Belfort, France*
*Author for Correspondence: richgille@gmail.com

ABSTRACT

In this article, we present the magnetic gears and more precisely the concentric magnetic reducer as a replacement for the mechanical gears given the limits of the latter. These limits are due to several factors such as friction and its inevitable lubrication (Gouda, 2011). The main goal we aim for is to study the insertion of magnetics reducers (MR) in permanent magnet synchronous machines (PMSM) for their design. Application fields of magnetics reducers being vast, we decided to apply it to an electric vehicle of the brand Renault ZOE. We kept the characteristics of the manufacturer and we replaced the electric propulsion system of the Renault ZOE with a magnetic reducer with incorporated a PMSM in a magnetically decoupled configuration. This propulsion system was made of a wound-rotor synchronous motor (WRSM) whose power was 65 kW. This was associated with a mechanical reducer that had a fixed reduction ratio equal to 9.32 (Krysinski, 2020) (Fodorean, 2016). We named this new system PMSM-MR. The electromagnetic sizing of the motor of this new system was presented as well as the sizing of the magnetic reducer. The model simulation on magnetostatic using the FLUX 2D software was carried out. The results obtained enabled us to approve the efficiency of this new system in static mode.

Keywords: Electric Propulsion, Electric Vehicle, Magnetic And Mechanical Reducers, Magnetically Decoupled Configuration, PMSM, Sizing, Magnetostatic Model, FLUX 2D

INTRODUCTION

The constant increase of oil price and concerns of natural environment protection, make that there is nowadays fast-growing interest in electric vehicle (EVs), globally (Chau, 2007) (Chan, 2001) (Wong, 2005). These vehicles offer promising solutions for sustainable transport, but their development is hampered by several technological challenges (Neuland, 1916) (Yao, 1997). To be competitive with internal combustion engines, EVs must offer the same dynamics, range, comfort conditions, and be cost-effective (Neuland, 1916) (Lee, 1985).

Components of the drive chain of EVs are the battery, the converter and the electrical propulsion. The electrical propulsion is composed of an electrical machine and a mechanical reducer. The largest share of losses is in the electrical propulsion (electrical machine and mechanical reducer), 72% (Fodorean, 2016). On the static converter, the loss is about 19%, and at the battery level, the loss is about 9% (Fodorean, 2016) Thereby, the autonomy range of electric cars is affected by the load capacity and the energy storage capability, which is directly influenced by the total weight of the car and the propulsion's efficiency (Larminie, 2012). Thus, a closer look at the propulsion system should be considered. Therefore, acting mainly on the electrical propulsion by improving its efficiency and power density will improve the overall autonomy of the electric vehicle (Neuland, 1916) (De Santiago, 2012) (Husain, 2011).

Using the mechanical reducer on EV affect the global power density of the traction system and its efficiency (Linni, 2010). This is due to the contact mechanism of the latter which generates losses, noise, vibrations and inevitable regular lubrication. In this context, the use of a magnetic traction system

Research Article

incorporating a PMSM and magnetic reducer that we name PMSM-MR could be the right solution. With this system, the engine can get rid of defects related to the mechanical gearbox. Besides, a highly integrated design can greatly reduce assembly size and weight.

The electric propulsion of the Renault ZOE vehicle is made of a wound-rotor synchronous motor (R 240) whose power was 65 kW. This latter is associated with a mechanical reducer that has a fixed reduction ratio equal to 9.32. His motor has a maximum speed of 11300 rpm and it provided a constant torque of 250 Nm up to 2500 rpm (Krysinski, 2020) (Fodorean, 2016). We gave ourselves the goal to replace the electric propulsion system of Renault ZOE by the PMSM-MR system which has the same characteristics. The sizing and simulation on FLUX 2D of this new PMSM-MR system to see its performance are presented in this article.

DESCRIPTION AND OPERATION OF THE PMSM-RM SYSTEM
PMSM-RM system (Figure 1) is composed of a synchronous motor with a permanent magnet with an external rotor incorporated in a concentric magnetic gear for obtaining a compact construction. The system has four mains parts: the motor stator, the outer rotor of the motor which is also the outer rotor of the reducer or the high-speed rotor, the ferromagnetic pole pieces and the outer rotor of the reducer or the low-speed rotor. This system contains three air gaps that are separated from each other.
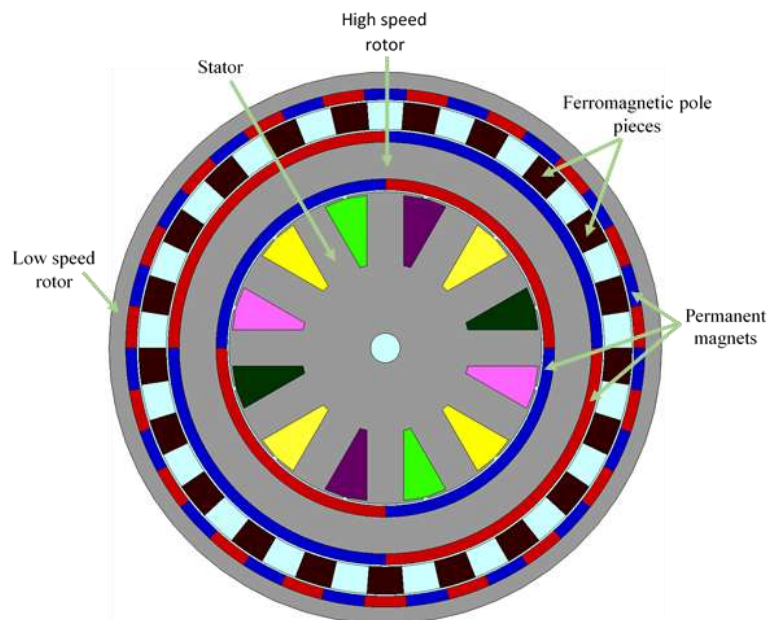
Figure 1: Representation of the PMSM-MR system

To magnetically isolate the magnetic reducer with flux modulation from the motor, the permanents magnets located in the inner and outer of the common of the PMSM and the magnetic reducer should be of opposing polarity. In this way, the electrical machine and the reducer can be magnetically decoupled. This configuration means that we have a thick common rotor making it possible to separate the fluxes of the reducer and the motor. Moreover, the decoupled configuration may be better suited to applications such as traction drives of EV (Gerber 2015).

The concentric magnetic reducer (Figure 2) is composed of two rotors one of which (inner rotor) is within the other (outer rotor) and a ring (stationary ring) consisting of ferromagnetic pole pieces located between the two rotors. Each rotor has on its surface (external for the inner rotor and internal for the outer rotor) a number of pairs of permanent magnet poles. Ferromagnetic pole pieces play an important role in the modulation of internal and external air gaps.

Research Article
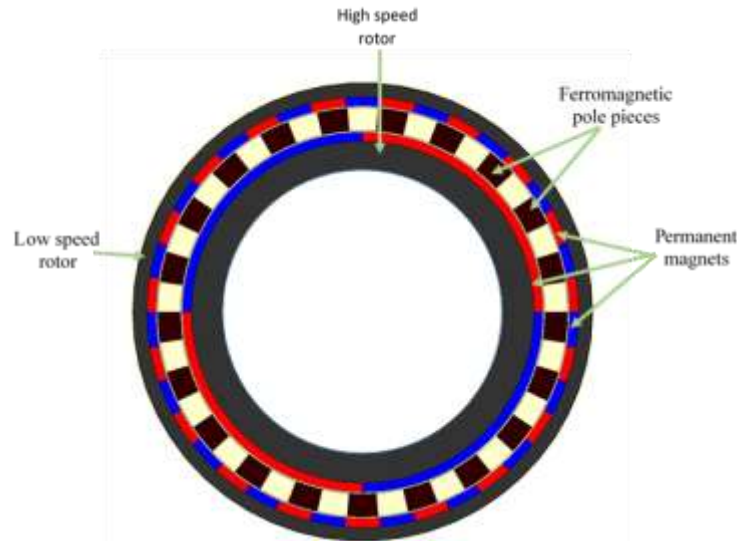
Figure 2: Representation of the concentric magnetic reducer

The number of ferromagnetic pole pieces and permanents magnets of concentric magnetic reducer satisfy the following relationship:

$$N_S = P_1 + P_2 \qquad (1)$$

where: P_1 and P_2 are respectively the number of pairs of permanent magnet poles of inner and outer rotor, N_S is the number of ferromagnetic pole pieces.

The G_r torque ratio can be defined by:

$$G_r = \frac{T_2}{T_1} = -\frac{P_2}{P_1} = -\frac{\omega_1}{\omega_2} \qquad (2)$$

where ω_1 and ω_2 are respectively the rotational speeds of the inner and outer rotors, T_2 and T_1 are the magnetic torques acting respectively on the outer and inner rotors.

The PMSM of the system (Figure 3) is at the salient pole. It consists of an internal stator and an external rotor.
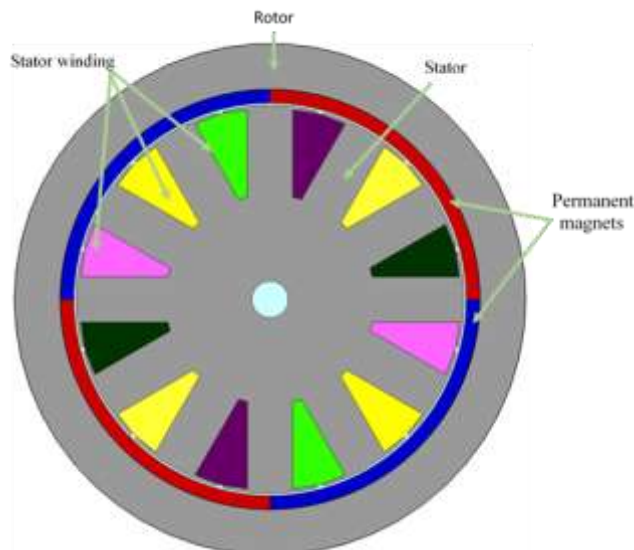
Figure 3: Representation of the MSAP of the system

When the stator of the PMSM is energized, it creates an electromagnetic torque that rotates the inner rotor (high-speed rotor) of the magnetic reducer. Thanks to the modulation of the magnetic flux by the

Research Article

ferromagnetic pole pieces, this torque is transmitted to the outer rotor (low-speed rotor) in the transmission ratio G_r of the PMSM-MR system.

SIZING OF THE PMSM-MR SYSTEM
The sizing of the system is based on the determination of the geometric parameters of the PMSM and the magnetic reducer. The system is magnetically decoupled, we separated the electromagnetic sizing of the PMSM and the magnetic reducer sizing. The geometric parameters of the PMSM to be determined are presented in figure 4 below.
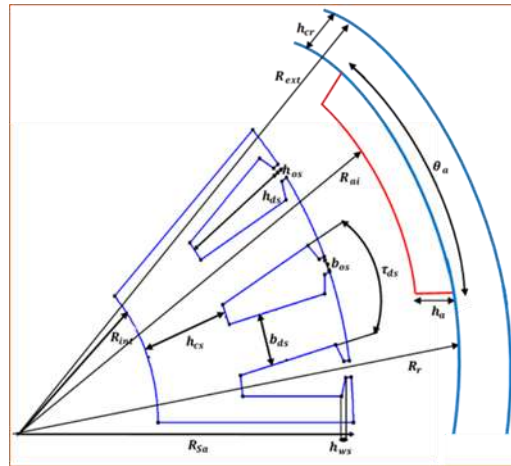
Figure 4: Geometric parameters of the system MSAP

Table 1: Geometric parameters of the PMSM obtained after dimensioning

PMSM's general setting	Nominal power	P_u	65 kW
	Number of phases	m	3
	Useful length	L_u	200 mm
Stator	Number of notches	Q_s	12
	Number of notches per pole and per phase	q_s	1
	Current density	J	4 A/mm^2
	Stator radius	R_{Sa}	84.88 mm
	The inner radius of the stator	R_{int}	8 mm
	Stator notch height	h_{ds}	38.11 mm
	Notch isthmus opening	b_{os}	2.5 mm
	Notch isthmus height	h_{os}	1 mm
	Height from top of notch isthmus	h_{ws}	1 mm
	Stator yoke height	h_{cs}	37.77 mm
Airgap	The thickness of the air gap	e	1 mm
Magnet	Material nuance	$NdFeB$	
	Outer radius	R_r	91.88 mm
	Inner radius	R_{ai}	85.88 mm
	Thickness	h_a	6 mm
	Angular opening relative to a pole	α_a	1
Rotor yoke	Outer radius	R_{ext}	111.88 mm
	Inner radius	R_r	91.88 mm
	Thickness	h_{cr}	20 mm

After a pre-sizing using the basic formulas of electromagnetism applicable to electric machines, we made the sizing of the PMSM. The parameters obtained after sizing are reported in table 1. We were able to

---

Research Article

obtain a PMSM with a power of 65 kW having two pairs of poles at the rotor and a useful length of 200 mm.

For the sizing of the magnetic reducer, we respect the specifications. As stated, the PMSM-MR system has a power of 65 kW, a maximum inner rotor speed of 11300 rpm and a fixed reduction ratio of 9.32. With these characteristics, the system can provide at the output of the reducer a maximum speed of 1212.44 rpm and a maximum torque $T_2 = 512$ N.m. We used this output data for the determination of the optimal geometric parameters of the magnetic reducer.

The number of pole-pairs P of the permanent magnets of the PMSM must be equal to the number of pole-pairs P_1 of the permanent magnets of the inner rotor of the reducer. This number was fixed at 2; then $P_1 = 2$.

The torque ratio of the magnetic reducer is $G_r = 9.32$. Equation 2 allows us to determine the number of pole-pairs P_2 of the outer rotor which is 18.64. Or this value must be an integer. We then round it up to the higher integer and we, therefore, find that $P_2 = 19$. Consequently one calculates again G_r which becomes $G_r = 9.5$ for the magnetic reducer.

The geometric parameters of the magnetic reducer to be determined are presented in figure 5, the results obtained are mentioned in table 2.
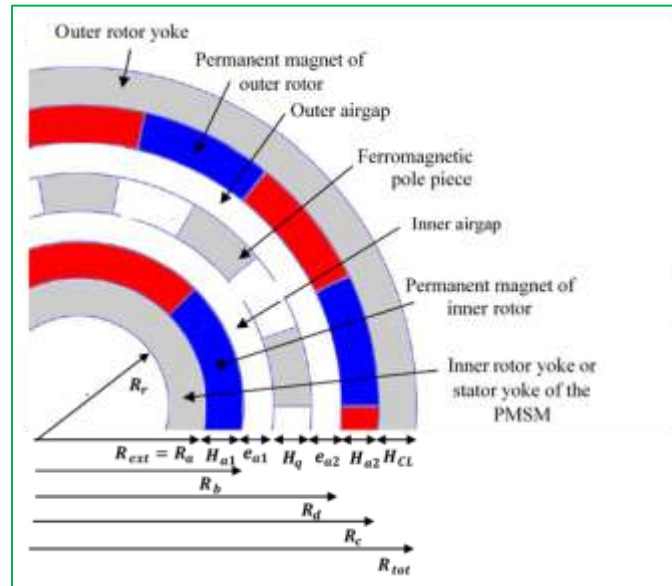
Figure 5: Geometric parameters of the magnetic reducer

Table 2: Geometric parameters of the magnetic reducer obtained after dimensioning

Number of pole-pairs on the inner rotor	P_1	2
Number of pole-pairs of the outer rotor	P_2	19
Number of ferromagnetic pole pieces	N_s	21
Thickness of inner air gap	e_{a1}	1 mm
Thickness of outer air gap	e_{a2}	1 mm
Thickness of ferromagnetic pole pieces	H_q	15 mm
Thickness of permanent magnets of the inner rotor	h_{a1}	6 mm
Thickness of permanent magnets of the outer rotor	h_{a2}	6 mm
Thickness of inner rotor yoke	h_{cr}	20 mm
Thickness of outer rotor yoke	H_{CL}	9.12 mm
Inside radius of reducer	R_a	111.88 mm
Outside radius of reducer	R_{tot}	150 mm
Useful length	L_u	200 mm

Research Article

ANALYSIS OF THE SIMULATION OF THE PMSM-RM SYSTEM

We carried out the magnetostatic simulation of the system under FLUX 2D. The distribution of field lines in the system is shown in figure 6. It is noted that the distribution of the flux creates the formation of 4 poles in the PMSM and which at the level of the magnetic reducer, the fields mainly pass through the ferromagnetic pole pieces.

Figure 7 shows the detailed mapping of magnetic induction throughout the system.

Table 3 below groups together the maximum values of the inductions in the three air gaps of the system (PMSM's air gap, inner and outer air gaps of the magnetic reducer) and the stator yoke, tooth and the rotor of the PMSM system.
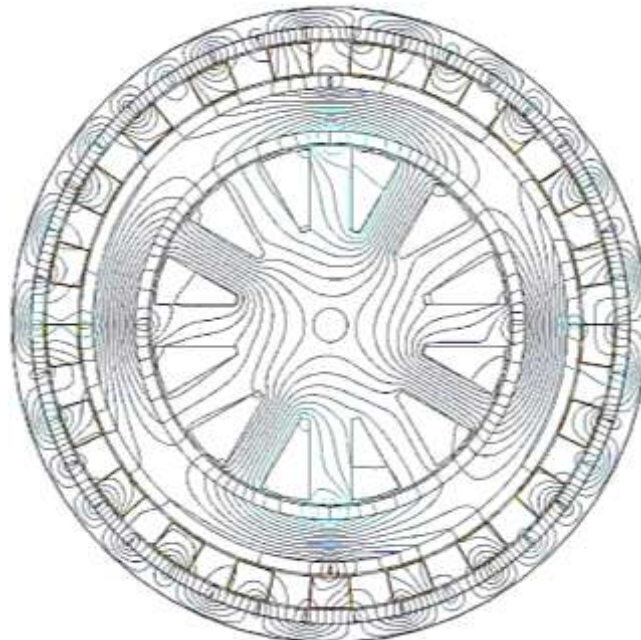
Figure 6: Distribution of field lines in the PMSM-MR system
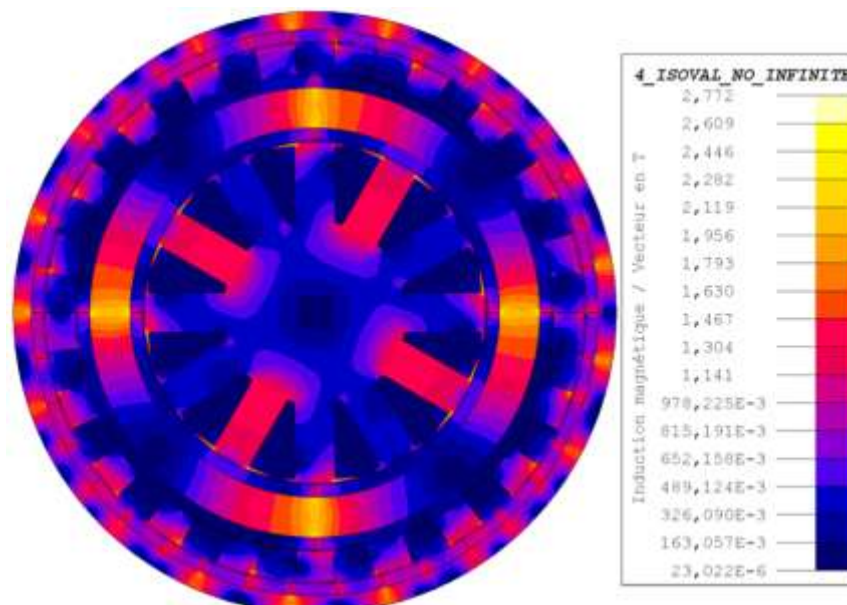
Figure 7: Detailed mapping of magnetic induction throughout the PMSM-MR system

Research Article

Table 3: Maximum induction in the different zones of the system

Zone of the PMSM-MR system considered	Maximum induction obtained by simulation	Chosen value for sizing	Induction limit for the salient pole PMSM
PMSM air gap	0.81 T	0.85 T	[0.8 T; 1.05 T]
Stator yoke	1.28 T		[1.1 T; 1.5 T]
tooth	1.91 T	1.9 T	[1.6 T ; 2.0 T]
PMSM rotor	1.97 T		[1.3 T; 1.6 T]
Inner air gap	1.17 T		
Outer air gap	1.6 T		

It is noted that the inductions at the yoke, the rotor, the teeth, and at the PMSM air gap are close to the values chosen for sizing and are included within the induction limits of the machine. Also, there is a slight saturation of the rotor yoke of the PMSM. This saturation contributes to the mechanical strength of the inner rotor and the correct magnetic operation of the PMSM-MR system. It also contributes to buckle again the flux of magnets. We also notice that the induction at the level of the outer air gap is greater than that of the inner air gap. Which allows having a high torque at the output of the magnetic reducer. Given these results, we can therefore conclude that the PMSM-MR system is effective in static mode.

CONCLUSION
In this article, we dimensioned a magnetic reducer integrated into a synchronous machine with a permanent magnet in accordance with the specifications that we defined beforehand. The determination of the geometric parameters of the PMSM-MR system enabled us to simulate the latter using the FLUX 2D software. The results obtained in magnetostatic being satisfactory, we then proved that the system can integrate well an electric vehicle. It can therefore replace the traction chain of any electronic vehicle fitted with a mechanical reduction gear while having the advantage of reduced mass and an intense magnetic field that can allow it to develop a high output torque moreover. To have a global view of the total efficiency of the system, we plan to study its behaviour according to the dynamic and thermal models.

REFERENCES
Chan CC and Chau KT (2001). Modern Electric Vehicle Technology. Oxford University Press, *Power Engineering Journal.*
Chau KT and Chan CC (2007). Emerging energy-efficient technologies for hybrid electric vehicles. *Proceedings of the IEEE.* **95**(4) 821−835.
De Santiago J *et al.,* (2012). Electrical motor drivelines in commercial all-electric vehicles: a review. *IEEE Transactions on Vehicular Technology*. **61**(2) 475–485.
Fodorean. D (2016). State of the Art of Magnetic Gears, their Design, and Characteristics with Respect to EV Application, in Modeling and Simulation for Electric Vehicle Applications. *In:* M. A. Fakhfakh, Éd. InTech., http://dx.doi.org/10.5772/64174.
Gerber S (2015). Evaluation and Design Aspects of Magnetic Gears and Magnetically Geared Electrical Machines. PhD Thesis, Stellenbosch University, 196.
Gouda EAA (2011). Transmission planétaire magnétique: étude, optimisation et réalisation. *PhD Thesis, Nancy* 1, 144.
Husain I (2011). Electric and hybrid vehicles: design fundamentals. 2nd edition. Boca Raton, Florida, USA: CRC Press.
Krysinski T and Malburet F (2020). Énergie et motorisation automobile et aéronautique. ISTE Editions Ltd (2020), https://patents.google.com/patent/US1171351A/en.
Larminie J and Lowry J (2012). Electric vehicle technology explained. 2nd edition, West Sussex, England: Wiley.

Research Article

Lee R, Brewer E and Schaffel N (1985). Processing of Neodymium-Iron-Boron melt-spun ribbons to fully dense magnets. IEEE Transactions on Magnetics. **21**(5) 1958-1963.

Linni J (2010). Design, Analysis, and Application of Coaxial Magnetic Gears. *PhD Thesis, University of Hong Kong,* 204.

Neuland AH (1916). Apparatus for transmitting power. *In:* U.S. Patent, 1 171 351, https://patents.google.com/patent/US1171351A/en.

Wong YS, Chau KT and Chan CC (2005). Load forecasting of hybrid electric vehicles under real-time pricing. *Journal of Asian Electric Vehicles*. **3**(2) 815-818.

Yao YD, Huang DR., Hsieh CC, Chiang DY and Wang SJ (1997). Simulation Study of the Magnetic Coupling Between Radial Magnetic Gears. *IEEE Transactions on Magnetics*. **33**(2) 2203–2206.